International Journal of General Medicine Dovepress

Open Access Full Text Article ORIGINAL RESEARCH

MiR-21-5p Modulates Cisplatin-Resistance of CD44+ Gastric Cancer Stem Cells Through Regulating the TGF-β2/SMAD Signaling Pathway

Xinyang Nie[1–3,*], Jian Liu[1,2,*], Daohan Wang[1,2,*], Chuan Li[1,2], Yuxin Teng[1,2], Zhufeng Li[1,2], Yangpu Jia[1,2], Peiyao Wang[1,2], Jingyu Deng[2,3], Weidong Li[1,2], Li Lu[1,2]

[1]Department of General Surgery, Tianjin Medical University General Hospital, Tianjin, People's Republic of China; [2]Tianjin Medical University, Tianjin, People's Republic of China; [3]Department of Gastric Surgery, Tianjin Medical University Cancer Institute and Hospital, National Clinical Research Center for Cancer, Key Laboratory of Cancer Prevention and Therapy, Tianjin, Tianjin's Clinical Research Center for Cancer, Tianjin, 300060, People's Republic of China

*These authors contributed equally to this work

Correspondence: Li Lu; Weidong Li, Department of General surgery, Tianjin Medical University General Hospital, 154, Anshan Road, Heping District, Tianjin, 300052, People's Republic of China, Email luli_1989@126.com; tjmughgs_lwd@163.com

Background: Cisplatin (DDP) resistance in gastric cancer (GC) is likely to come from gastric cancer stem cells (GCSC). It is a new idea to study the mechanism of the DDP-resistance in GCSC from miRNA.

Materials and Methods: CD44+ GCSCs and CD44- control cells were constructed based on the HGC27 gastric cancer cell line. DDP sensitivities in CD44+ and CD44- cells were detected via CCK-8 assay. The differential expression of miR-21-5p in these cell lines was detected by RT–qPCR. The expression levels of downstream TGF-β2, SMAD2 and SMAD3 were determined through RT–PCR and Western blotting. A luciferase assay was used to detect the relationship between miR-21-5p and TGFB2, and the TCGA database, clinical data from our centre, and vivo experiment were used for validation. Finally, we knocked down miR-21-5p to detect changes in cisplatin resistance in GCSCs and to verify changes in the levels of downstream pathways in GCSCs.

Results: CD44+ GCSCs induced cisplatin resistance compared with CD44- cells. miR-21-5p was highly expressed in GCSCs, and the TGF-β2/SMAD pathway was also highly expressed. TGFB2 was proven to be a downstream target gene of miR-21-5p and had a positive relationship with it in phenotype. After knockdown of miR-21-5p, the TGF-β2/SMAD pathway was also inhibited, and the resistance of GCSCs to cisplatin was specifically decreased.

Conclusion: MiR-21-5p promotes cisplatin resistance in gastric cancer stem cells by regulating the TGF-β2/SMAD signalling pathway.

Keywords: miR-21-5p, cisplatin resistance, GCSCs, TGF-β2 pathway

Introduction

Gastric cancer (GC) is a very common malignant tumour that ranks fifth in incidence among the major types of cancer globally (5.6%), with 1,089,103 new cases per year, and is the fourth leading cause of cancer-related death (7.7%), with 768,793 deaths worldwide.[1] Cancer stem cells (CSCs), which have primitive stem cell properties as well as malignant characteristics, are being studied by an increasing number of researchers.[2] Emerging evidence suggests that CSCs may play a pivotal role in cancer progression and treatment resistance in GC.[3] They are distinguished by their self-renewal capacity, chemoresistance, and heightened potential for metastasis through epithelial-mesenchymal transition (EMT), making them highly significant therapeutic targets.[4–6] As a result, one of the most effective strategies for identifying and eliminating CSCs is to target several cell surface markers overexpressed in CSCs.[7,8] CD44, a transmembrane glycoprotein, is one of the recognized gastric cancer stem cell (GCSC) markers and is used to isolate CSCs in various cancers, particularly in GC.[9–11]

Received: 26 June 2024
Accepted: 3 October 2024
Published: 11 October 2024

Chemotherapy is an important treatment for GC, and cisplatin (DDP), a platinum compound, is frequently adopted as a first-line drug in the treatment of GC, which was discovered and first used in the 1840s. Cisplatin induces apoptosis by binding to and crosslinking DNA.[12] In advanced gastric cancer, combination chemotherapies that include cisplatin have been shown to improve survival times and response rates.[10,13] However, chemoresistance of tumours is a major impediment to chemotherapy and one of the primary causes of its failure.[14] Recent evidence suggests that stem-like phenotypes in cancer cells, which are promoted by CSCs, are the main culprit of chemoresistance. Many mechanisms have been proposed for CSC resistance, such as overactivation of the DNA damage response (DDR), apoptosis evasion, drug efflux through ABC transporters, prosurvival pathway activation, cell cycle promotion and/or cell metabolic alterations.[15,16]

Microribonucleic acids (miRNAs) are endogenous and small noncoding RNA molecules (~22 nt), and their involvement in cancer has been widely studied. Some miRNAs may inhibit or promote cancer cells, and they also play a great role in the drug resistance of cancer by altering downstream gene expression.[17] Moreover, miRNAs play an important role in modulating CSC properties, such as self-renewal capacity, migration and invasion, and chemoresistance.[18–20] Pan Y et al[19] reported that miR-196a-5p modulated GCSC characteristics by targeting Smad4. Ma C et al[21] indicated that miR-200c overexpression inhibited chemoresistance, invasion and colony formation in pancreatic CSCs.

In this study, we identified CSC phenotypes in CD44(+) stem-like cells in GC. We subsequently analysed the miRNA expression profiles of CD44(+) and CD44(-) gastric cells to investigate the molecular mechanisms underlying CSC characteristics. Our analysis revealed that miR-21-5p was significantly differentially expressed between the two cell types. In a previous experiment, we found that miR-21-5p was also highly expressed in gastric cancer patients with high CD44 expression. At the same time, miR-21-5p was reported to be associated with drug resistance in multiple types of cancer, including breast cancer,[22] hepatoma,[23] lung cancer,[24] colorectal carcinoma,[25] gastric cancer[26,27] and others.[28] Thus, we speculated that miR-21-5p may play an important role in the DDP resistance of GCSCs, and we therefore sought to provide a new therapeutic avenue for gastric cancer.

Materials and Methods

Cell Lines and Cancer Stem Cell Culture

Serum-free medium (SFM) was composed of DMEM/F12 (Thermo Scientific), 2% B27 supplement (Thermo Scientific), 1% N-2 supplement (Thermo Scientific), 10 ng/mL basic fibroblast growth factor (bFGF, PeproTech, USA), 20 ng/mL epidermal growth factor (EGF, PeproTech) and 1% penicillin–streptomycin sulfate (Thermo Scientific). GCSCs were isolated from the HGC27 cell line and formed sphere-like cell aggregates by using SFM. HGC27 cells were obtained from MeisenCTCC Co., Ltd. (Zhejiang, China). All cultures were maintained in a 37 °C incubator supplemented with 5% CO_2.

Flow Cytometry Analysis and Fluorescence-Activated Cell Sorting

For flow cytometry, cells at approximately 80% confluence in a 100-mm plate were washed with PBS. Cells were then detached from plates using trypsin-EDTA and centrifuged at 4 °C. The cells were stained with a 400-fold dilution of anti-CD44-FITC (Thermo Scientific) and incubated for 1 h at 4 °C. Then, the cells were washed with PBS. Finally, they were analysed and sorted immediately with fluorescence-activated cell sorting (FACS) AriaIII (BD Biosciences). At least 10,000 cells were analyzed for each experiment. A rough live / dead gate was set on the forward divergence (FSC) / lateral divergence (SSC) histogram, and then single-cell gating of these cells was performed using SSC height and SSC area. Stricter exclusion of dead cells was achieved by excluding propidium iodide (PI) -positive cells from singlet-gated cells. Finally, CD44-and CD44+ groups were screened out according to 10% before and after FITC staining for subsequent experiments.

MiRNA Sequencing and Data Analysis

Transcriptome sequencing and analysis were performed by Gene Denovo Biotechnology Company (Guangzhou, China). Total RNA was extracted using TRIzol reagent (Thermo Scientific) according to the manufacturer's instructions, and the

RNA molecules measuring 18–30 nucleotides were enriched by polyacrylamide gel electrophoresis. The library was constructed using an NEBNext® Multiplex Small RNA Library Prep Kit for Illumina (E7300; New England BioLabs, Inc., MA, USA). The 3′ adapters were then added, and the 36–44 nucleotide RNAs were enriched; the 5′ adapters were then ligated to the RNAs. The ligation products were reverse-transcribed by PCR amplification, and the 140–160-base-pair PCR products were enriched to generate a cDNA library. The quality of the library was assessed on a Bioanalyzer 2100 system (Agilent Technologies Inc., CA, USA), and an ABI StepOnePlus Real-Time PCR System (Life Technologies Inc., CA, USA) was used for quantification. A 3 nM cDNA library was sequenced from 5′ to 3′ using an Illumina HiSeq 2500 SE50 with a sequencing strategy of single-end 50 bp reads (Illumina Inc., CA, US). Libraries were then amplified and sequenced using Illumina Novaseq6000 by Gene Denovo Biotechnology Co. The procedure was performed as previously described.

Total miRNAs consists of existing miRNA, known miRNA and novel miRNA based on their expression in each sample. The miRNA expression level was calculated and normalized to transcripts per million. miRNAs with a fold change of ≥2 and P <0.05 in a comparison were identified as differentially expressed miRNAs. RNAhybrid, Miranda, TargetScan and miRBase were used to predict the target genes of the existing miRNAs, known miRNAs and novel miRNAs, and the functions of miRNA target genes were analysed via functional enrichment analysis.

TCGA Database Analysis

We obtained high-throughput sequencing data of gastric cancer from TCGA-STAD (The Cancer Genome Atlas-Stomach Adenocarcinoma). As logFC > 1 and p <0 0.05 were defined as the standard of DEGs, we acquired DEGs through the limma R and edgeR packages. The differentially expressed miRNAs in cancer and normal tissues from the database were analysed, and the target miRNAs and mRNAs were grouped and compared simultaneously.

Cell Counting Kit-8 (CCK-8) Assay

Cells in the logarithmic growth phase were uniformly inoculated into a 96-well plate (1×10^4/well) and cultured in an incubator for 24 h. After 48 h of induction with different concentrations of DDP, 190 μL of fresh medium containing 10 μL of CCK-8 reaction solution (Yeasen Biotechnology, Shanghai, China) was replaced, followed by incubation in the dark at 37 °C for 2 h. The absorbance at 450 nm was detected using a microplate reader, and the IC50 of cisplatin was calculated.

Quantitative Real-Time PCR (qRT–PCR)

Total RNA was extracted from cells using TRIzol reagent (Vazyme Biotech, Nanjing, China) according to the manufacturer's instructions. First-strand cDNA was synthesized using oligo(dT) primers and HiScript III reverse transcriptase (Vazyme). Real-time PCR was carried out with a PCR mixture containing each primer (1 μM) and ChamQ Universal SYBR qPCR Master Mix (Vazyme). Thermocycling conditions included incubations at 95 °C for 10 seconds and 60 °C for 30 seconds, which were carried out using a CFX96 real-time PCR machine (BIO-RAD, USA). Each sample was examined in triplicate, and the amount of PCR product was normalized with respect to GAPDH as an internal control. The real-time PCR primers are shown in Table 1.

cDNA for the miRNA assay was synthesized using TransScript miRNA First-Strand cDNA Synthesis SuperMix (TransGen Biotech, Beijing, China) with miR-21-5p and U6-specific primers (Synbio Technologies, Suzhou, China) according to the manufacturer's instructions. Real-time PCR for miRNA quantification was carried out with the PerfectStart Green qPCR SuperMix (TransGen). The amplifications were conducted at 94 °C for 5 seconds and at 60 °C for 30 seconds using a CFX96 real-time PCR machine (BIO-RAD). Each sample was examined in triplicate, and the amount of PCR product was normalized with respect to U6 as an internal control. PCR amplification of miRNA-reversed cDNA was carried out by using Phanta Flash Master Mix (Vazyme). Standards were prepared after purification of cDNA by using the FastPure Gel DNA Extraction Mini Kit (Vazyme). Tenfold serial dilutions over five points were prepared from the cDNA, and they were then used as templates for qPCR. The standard curve was constructed by plotting Cq values against the logarithmic concentration of the calibrator oligoribonucleotides. The amount of an unknown sample was quantified by interpolating the Cq values in the standard curve.

Table 1 The Real-Time PCR Primers of Different Genes

Gene	Direction	Primer Sequences (5'-3')
Has-miR-21-5p		TAGCTTATCAGACTGATGTTGAGCC
U6		GCTTCGGCAGCACATATACTAAAAT
TGFB2	F	CAGCACACTCGATATGGACCA
	R	CCTCGGGCTCAGGATAGTCT
SMAD2	F	CGTCCATCTTGCCATTCACG
	R	CTCAAGCTCATCTAATCGTCCTG
SMAD3	F	CCATCTCCTACTACGAGCTGAA
	R	CACTGCTGCATTCCTGTTGAC
GAPDH	F	CTCCTCCACCTTTGACGCTG
	R	TCCTCTTGTGCTCTTGCTGG

miRNA Inhibitor Transfection

A microRNA inhibitor was purchased from Synbio Tech. Cells were seeded into six-well plates and incubated overnight. The cells were transfected with siRNA as a miR-21-5p inhibitor (UCAACAUCAGUCUGAUAAGCUA) and negative control (UCUACUCUUUCUAGGAGGUUGUGA) using Lipofectamine 2000 (Invitrogen) according to the manufacturer's instructions. After 48 or 72 hours, the cells were harvested for RNA and protein isolation.

Luciferase Reporter Assay

The 3'-UTR of TGFB2 containing miR-21-5p seed binding sites was cloned into the psiChECK-2 vector to construct the wild-type (WT) vector. A mutant 3'-UTR of TGFB2 was synthesized by PCR and cloned into the psiChECK-2 vector to construct the mutation type (Mut) vector. Cells were seeded into six-well plates and incubated overnight. The cells were cotransfected with TGFB2-WT/mut destination plasmid or miR-21-5p inhibitor/NC according to the manufacturer's instructions. After 48 hours, the luciferase activity of the cell lysates was measured using the Dual Luciferase Reporter System (Promega). Luminescence was measured with a Glomax luminometer (Promega). The results are expressed as the averages of the ratios of the activities from triplicate experiments. Renilla luciferase activities were standardized to firefly luciferase activities.

Protein Extraction and Western Blot Analysis

The cells were lysed in an appropriate amount of RIPA lysis buffer containing protease inhibitor (Thermo) and phosphatase inhibitor (Thermo). After centrifugation at 14000 rpm at 4 °C for 30 min, the protein supernatant was collected. The protein concentration was detected using a BCA protein assay kit (Epizyme, Shanghai, China). The protein was subjected to a heating bath at 95 °C for 10 min for protein denaturation. Samples were loaded into 8% sodium dodecyl sulfate–polyacrylamide gel electrophoresis (SDS–PAGE) gels and blotted onto polyvinylidene difluoride (PVDF) membranes. The PVDF membranes were immersed in Tris-buffered saline and Tween-20 (TBST) containing 5% skim milk powder and shaken slowly for 1 h. Then, the protein was incubated for 16 h with the primary antibody diluted with 1% BSA, rinsed with TBST 3 times (10 min/wash), and incubated again with the secondary antibody at room temperature for 1 h. Finally, the protein was detected using enhanced chemiluminescence (ECL) reagent, followed by exposure in a dark room. The relative expression of the protein was analysed using ImageJ, with β-actin as an internal reference.

Immunohistochemistry Assay

The paraffin-embedded tissues were sectioned at a thickness of 5 μm, and the sections were dewaxed in xylene and dehydrated in alcohol. After achieving antigen retrieval, the peroxidase activity was blocked with 3% H_2O_2 for 15 min. The primary antibodies against CD44 (1:150, Boster, Wuhan, China) and TGFβ2 (1:200, Proteintech, Wuhan, China) were added and incubated at 4 °C overnight, and the secondary antibody was incubated at room temperature for 1 hour. All slides were detected with a DAB kit (ZSGB-Bio, Beijing, China) and counterstained with haematoxylin. The sections were scored by the intensity of cell staining and the range of positive cells and finally multiplied to obtain the IHC score.

In vivo Xenograft and Treatment Experiments

For in vivo studies, 5 week-old female BALB/c nude mice were purchased from Charles River Laboratories of Beijing, China. CD44+ HGC27 and CD44- HGC27 cells (2× 10^6 cells in 100ul PBS) were subcutaneously injected into the nude mice to establish tumours. After 13 days, 5 mg/kg DDP or normal saline was injected intraperitoneally every 3 days. The mice were examined every 3 days and sacrificed 15 days after the first DDP treatment. The tumour sizes were measured using digital caliper and tumour volume was calculated with the following formula: volume = 0.52 × width2 × length. All animal procedures were carried out with the approval of the Institutional Committee of Tianjin Medical University for Animal Research. This study was conducted following the Animal Research: Reporting of in vivo Experiments (ARRIVE) guidelines and conformed with the Declaration of Helsinki.

Statistical Analysis

GraphPad Prism 9 software was used for the statistical analysis. The numerical data are presented as the means ± standard deviation (SD) of at least three determinations. Statistical comparisons between groups of normalized data were performed using the *t* test or Mann–Whitney *U*-test according to the test conditions. A p value < 0.05 was considered statistically significant with a 95% confidence level.

Results

CD44 is Significantly Upregulated in GCSCs

CD44 is known to be a surface marker of GCSCs. To obtain GCSCs, we performed fluorescence-activated cell sorting for CD44 on HGC27 cells. Approximately 10% of the cells with high CD44 expression were selected and considered CD44 +, while approximately 10% with low expression were used as controls. (Figure 1A) Next, we induced stemness culture of CD44+ cells to grow them in suspension and into spheres. (Figure 1B and C) CD44 was significantly highly expressed in CD44+ cells, which was verified by flow cytometry, PCR, and Western blotting. (Figure 1D–F) We also considered this batch of cells to be GCSCs.

CD44+ Cells Have Higher Cisplatin Resistance in vitro and in vivo

We conducted CCK-8 assays to examine the proliferative capacities of CD44- and CD44+ cells upon cisplatin treatment. After 48 hours of treatment with different concentrations of cisplatin, different viabilities were observed for CD44- and CD44+ cells. The half maximal inhibitory concentration (IC50) of CD44+ cells was significantly higher than that of CD44- cells, indicating that CD44+ cells had higher cisplatin resistance. (Figure 2A) To demonstrate DDP resistance of GCSCs in vivo, CD44+ and CD44- cells were injected subcutaneously into female nude mice for tumorigenesis, followed by DDP treatment and normal saline (0.9% NaCl) was used as a negative control. We found that the final tumour size of CD44+ group was 315.9±52.89 mm^3 after DDP treatment, which was significantly larger than that of CD44- group (122.0±54.69 mm^3). (Figure 2B) In addition, the mean tumour weight in CD44+ group was about 1 time heavier than that in CD44- group after DDP treatment. (Figure 2C) Taken together, these results suggested that GCSCs showed high resistance to DDP both in vitro and in vivo.

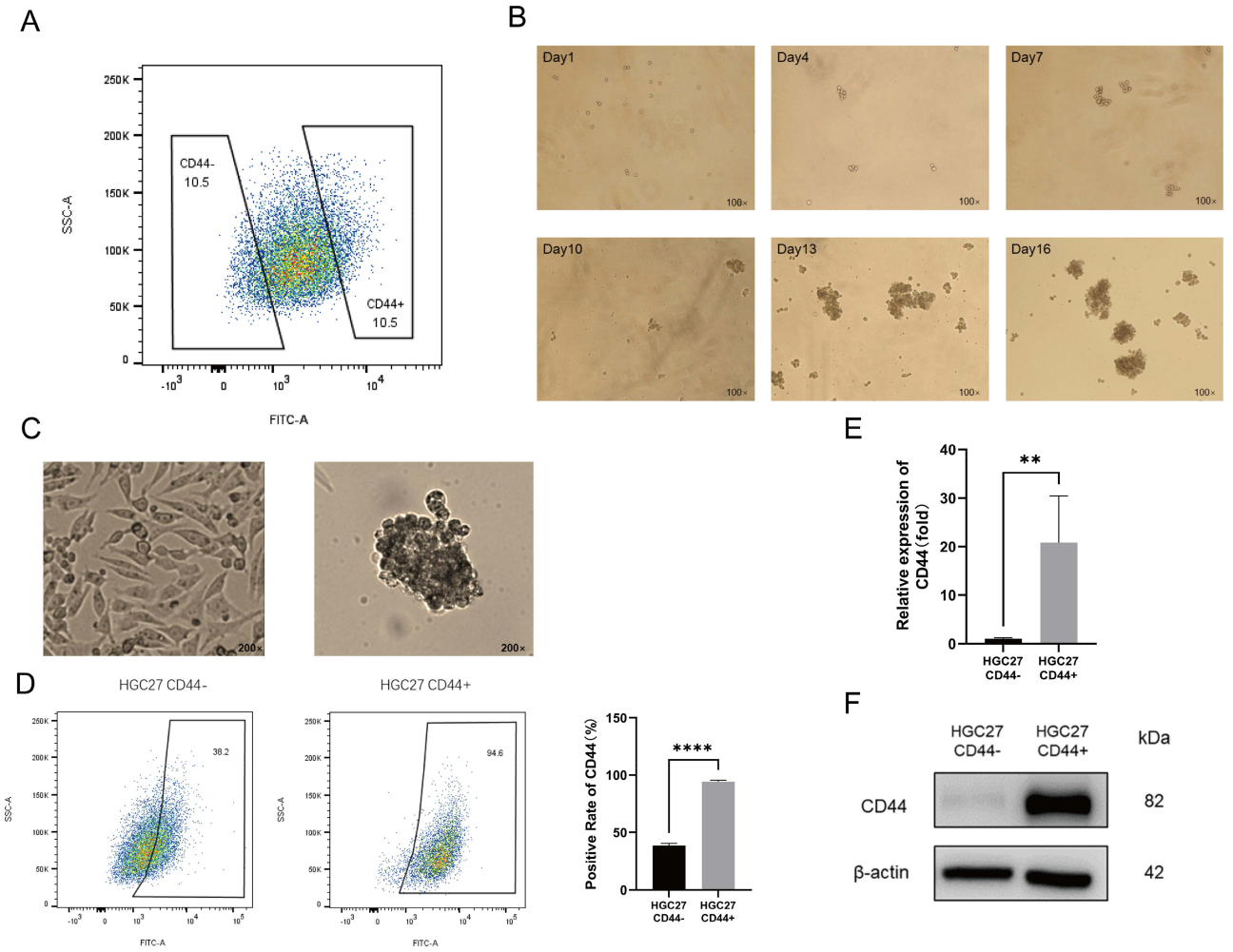

Figure 1 CD44 is significantly upregulated in GCSCs. (**A**) The expression of CD44 in HGC27 was analysed by flow cytometry, and about 10% of the upper and lower sides were selected to construct CD44- and CD44+ cell populations by fluorescence-activated cell sorting. (**B**) CD44+ cells were grown in stemness-culture, and the cells gradually changed from single cells to clusters and finally to spheres of cells over time. (**C**) Under 200x light microscope, HGC27 CD44- grows adherently, while CD44+ suspends into spheres. (**D**) The positive rate of CD44 in the CD44+ group by flow cytometry was about 95%, while it was about 40% in CD44- group, and there was a statistical difference between them. The quantitative data were presented as the mean ± SD of triplicate experiments. (****p < 0.0001) (**E**) Real-time PCR analysis of the CD44 expression level in CD44- and CD44+ cells and it was normalized by GAPDH and presented as the relative ratio. (**p < 0.01) (**F**) Western blot analysis of CD44 expression in CD44- and CD44+ cells.

MicroRNA-21-5p is Upregulated in CD44+ Cells

Transcriptome sequencing and analysis were performed on the two groups of cells, and we found that miR-21-5p was significantly upregulated in CD44+ cells (logFC=1.35, P<0.001) compared with CD44- cells. (Figure 3A and B) To validate our miRNA array data, the dataset from the TCGA database was analysed first. The data were divided into two sample groups according to the level of CD44 to simulate stem cells and nonstem cells in gastric cancer. MiR-21-5p had specific high expression in samples with high CD44 expression. (Figure 3C) For further validation, we collected 88 gastric cancer tissue samples in our centre. By immunohistochemical (IHC) staining, we used the score to represent the CD44 level of the samples. (Figure 3D) Scores ≥ 4 were considered samples with high CD44 expression, and scores ≤ 3 were considered samples with low expression. (Figure 3E) At the same time, absolute quantitative PCR was performed on the samples to examine the expression level of miR-21-5p. The result was the same as before. (Figure 3F) Finally, real-time PCR was performed on CD44+ and CD44- cells in vivo and in vitro. The high expression pattern of miR-21-5p in CD44+ cells was consistent with previous studies. (Figure 3G and H)

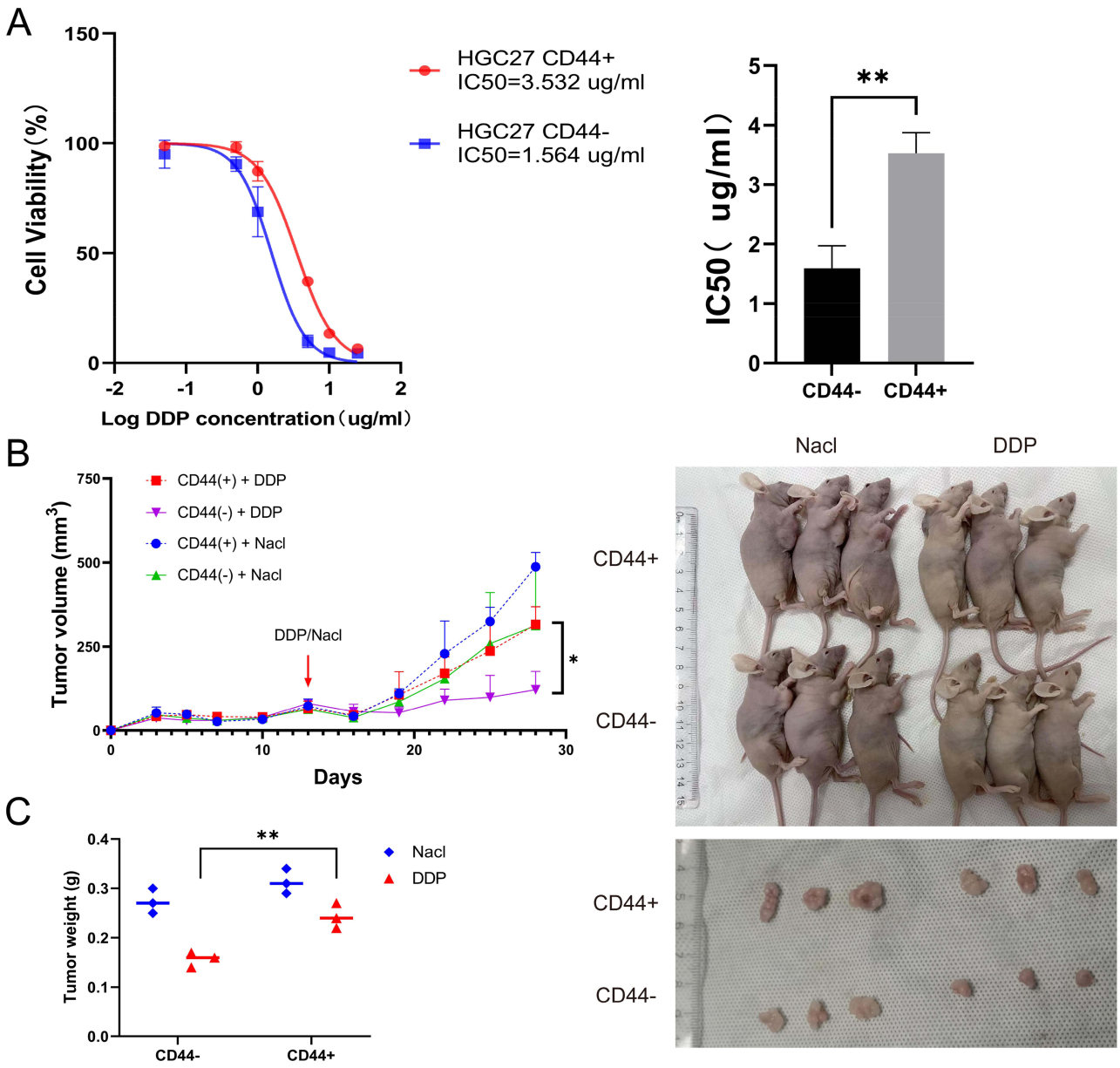

Figure 2 Cisplatin resistance in CD44+ and CD44- HGC27 cells in vitro and in vivo. (**A**): Viabilities of CD44+ and CD44- cells after treatment with different concentration cisplatin as measured by CCK8 assay. Values shown represent averages of half maximal inhibitory concentration; each treatment was carried out in triplicate (**p < 0.01). (**B**): Tumour growth curves in nude mice inoculated with HGC27 CD44- and HGC27 CD44+ cells that were treated by DDP (*p < 0.05). (**C**): The mean weight (left) and the size (right) of tumours at the end of the experiment from mice treated with DDP (**p < 0.01).

TGFB2 is a miR-21-5p Target Gene

Next, we investigated the candidate targets of miR-21-5p by RNAhybrid, Miranda, TargetScan, and miRbase. We found that TGFB2 was both a target gene associated with tumour and drug resistance by KEGG enrichment analysis and a differentially expressed gene based on transcriptome sequencing. Based on the bioinformatics prediction, there was a binding site in the 3'-UTR of TGFB2 mRNA targeted by miR-21-5p. (Figure 4A) To obtain further direct evidence that miR-21-5p alters TGFB2 expression, we performed luciferase reporter assays. MiR-21-5p can negatively regulate the expression of luciferase with the TGFB2 3'UTR, and this regulatory relationship largely disappeared after the binding site mutation. (Figure 4B) To confirm the relationship between the two, TCGA data were used to verify that the expression levels of miR-21-5p and TGFB2 were positively correlated in the gastric cancer database samples.

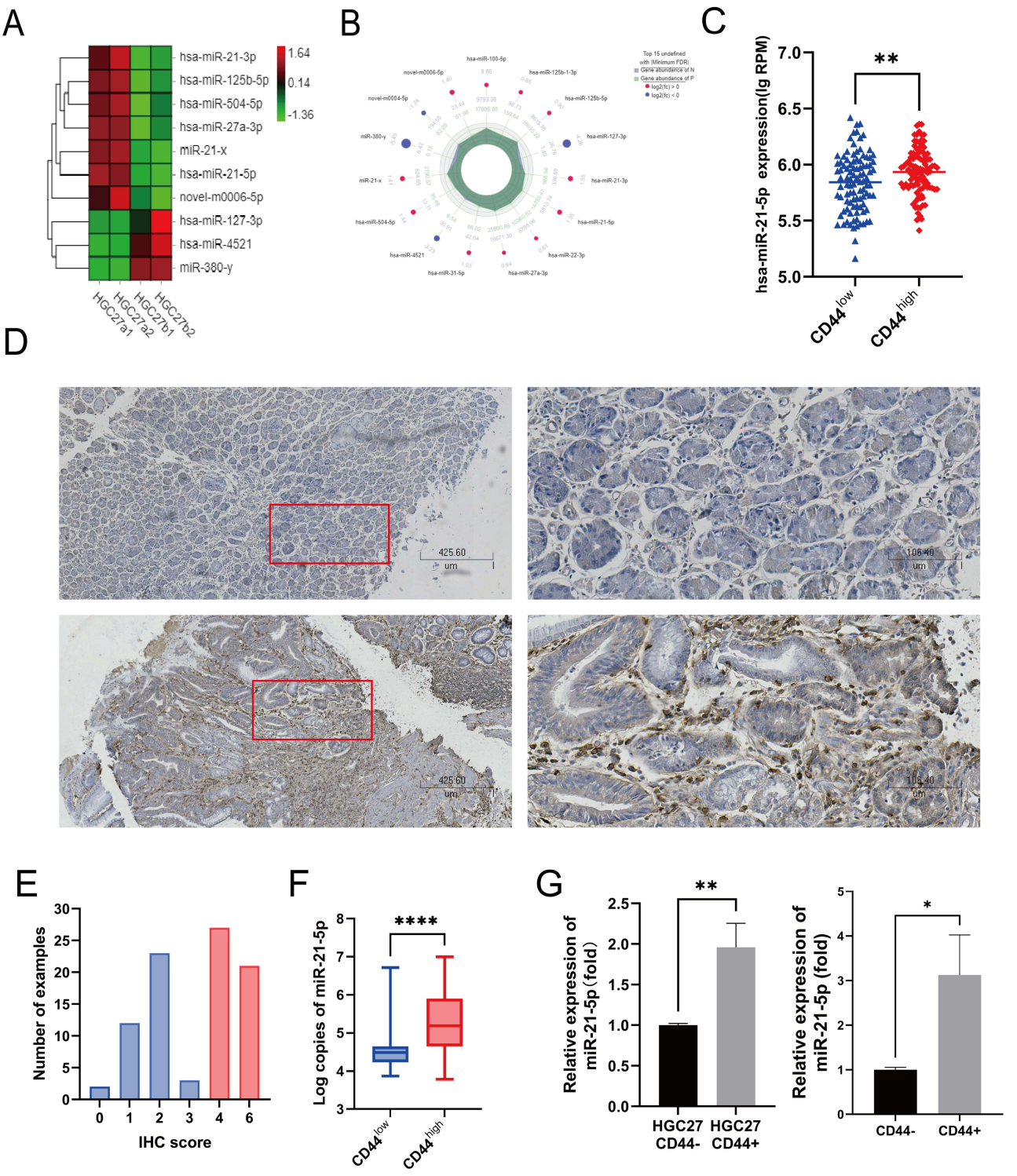

Figure 3 MicroRNA-21-5p is upregulated in CD44+ cells. (**A**): miRNA sequencing between HGC27 CD44- and CD44+ cells and the differentially expressed miRNAs were screened in the heatmap. Among them, HGC27a represented CD44+ HGC27 cells, while HGC27b represented CD44- HGC27 cells. (**B**): The radar chart showed the 15 miRNAs with the largest log ford change (logFC) differences between the two groups and llogFC of miR-21-5p was 1.35 ($p < 0.001$). (**C**): Expression levels of miR-21-5p between the two groups of samples with differential expression of CD44 in TCGA database. (**$p < 0.01$) (**D**): IHC staining of CD44 under electron microscope, and field of view at 50x (left) and 200x (right) respectively. Here we show the weak positive CD44 (above) as well as the strong positive CD44 (below). (**E**): Distribution of IHC scores forD44. According to the median CD44 score of 88 samples, they were divided into two groups, which were CD44 low and CD44 high. (**F**): The miR-21-5p expression levels between two groups of clinical samples by absolute quantitative PCR. (****$p < 0.0001$) (**G**): Real-time PCR analysis of the miR-21-5p expression level in HGC27 CD44- and HGC27 CD44+ cells in vitro (left) and in vivo (right). It was normalized by U6 and presented as the relative ratio. (*$p < 0.05$, **$p < 0.01$).

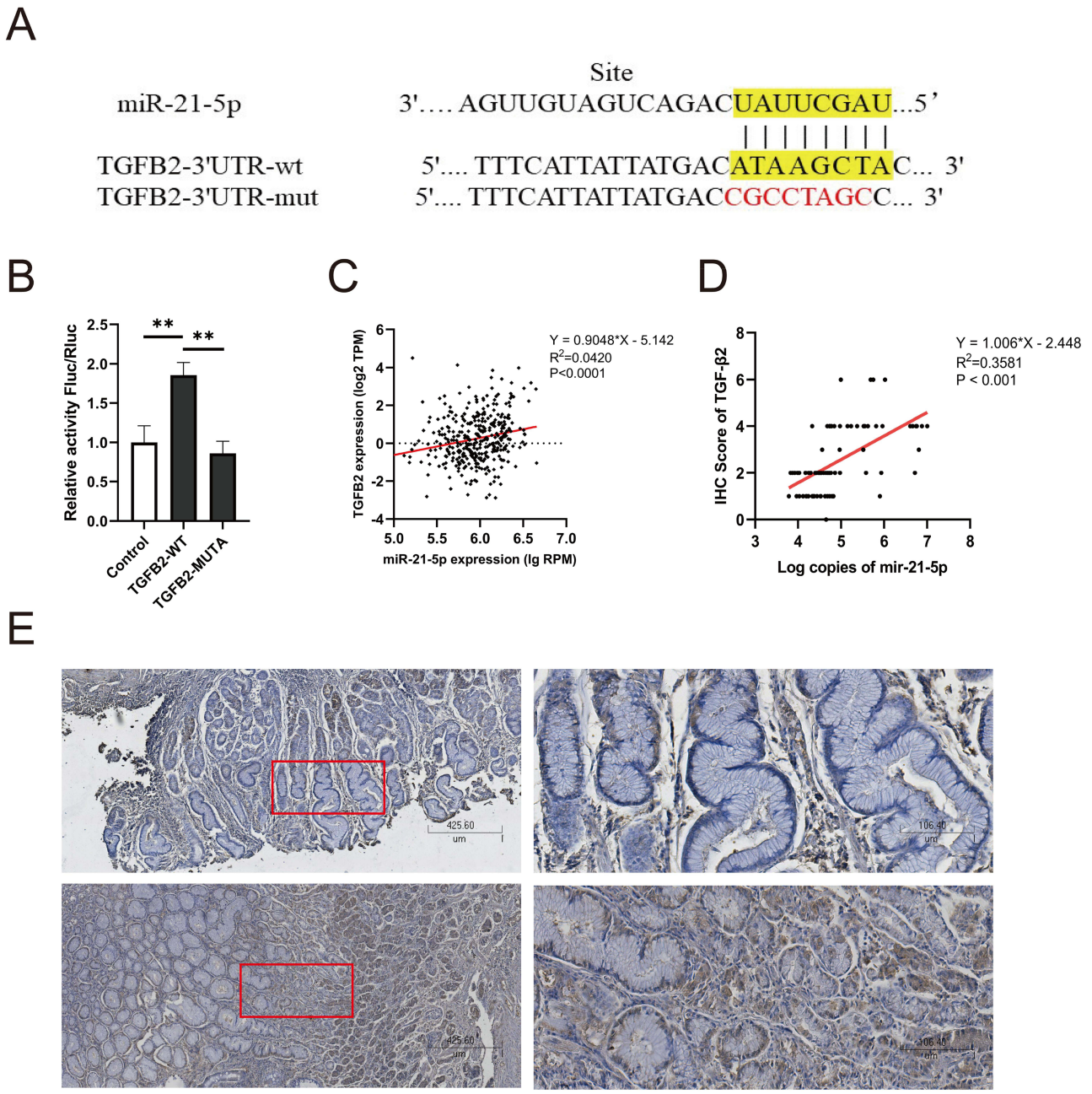

Figure 4 TGFB2 is a miR-21-5p target gene. (**A**): Putative miR-21-5p binding sequences in the 3'-UTR of TGFB2 mRNA. (**B**): Luciferase activity assay to examine the activity of TGFB2 in negative control or miR-21-5p inhibitor- transfected 293T cells. Data are expressed as a ratio of Firefly luciferase activity to Renilla luciferase activity (** p<0.01). (**C**): It showed a relationship between miR-21-5p and TGFB2 expression levels in samples in the TCGA database, and there was a positive correlation between the two fittings. (p < 0.0001) (**D**): The positive relationship between the log copies of miR-21-5p and the IHC staining score of TGF-β2 in clinical samples. (p < 0.001) (**E**): IHC staining of TGF-β2 under electron microscope, and field of view at 50x (left) and 200x (right) respectively. Here we show the weak positive TGF-β2 (above) as well as the strong positive TGF-β2 (below).

(Figure 4C) Remarkably, after IHC staining of clinical samples, we found that the expression of TGF-β2 in tumour tissue increased with the expression of miR-21-5p. (Figure 4D and E)

The TGF-β2/SMAD Signalling Pathway is Upregulated in CD44+ Cells

In the sequencing results, the expression level of TGFB2 was significantly higher in CD44+ cells than in CD44- cells. (Figure 5A) We obtained consistent conclusions in the TCGA database. (Figure 5B) In the IHC results of clinical samples, the expression level of TGF-β2 is displayed in a scored manner. There was a significantly elevated TGF-β2

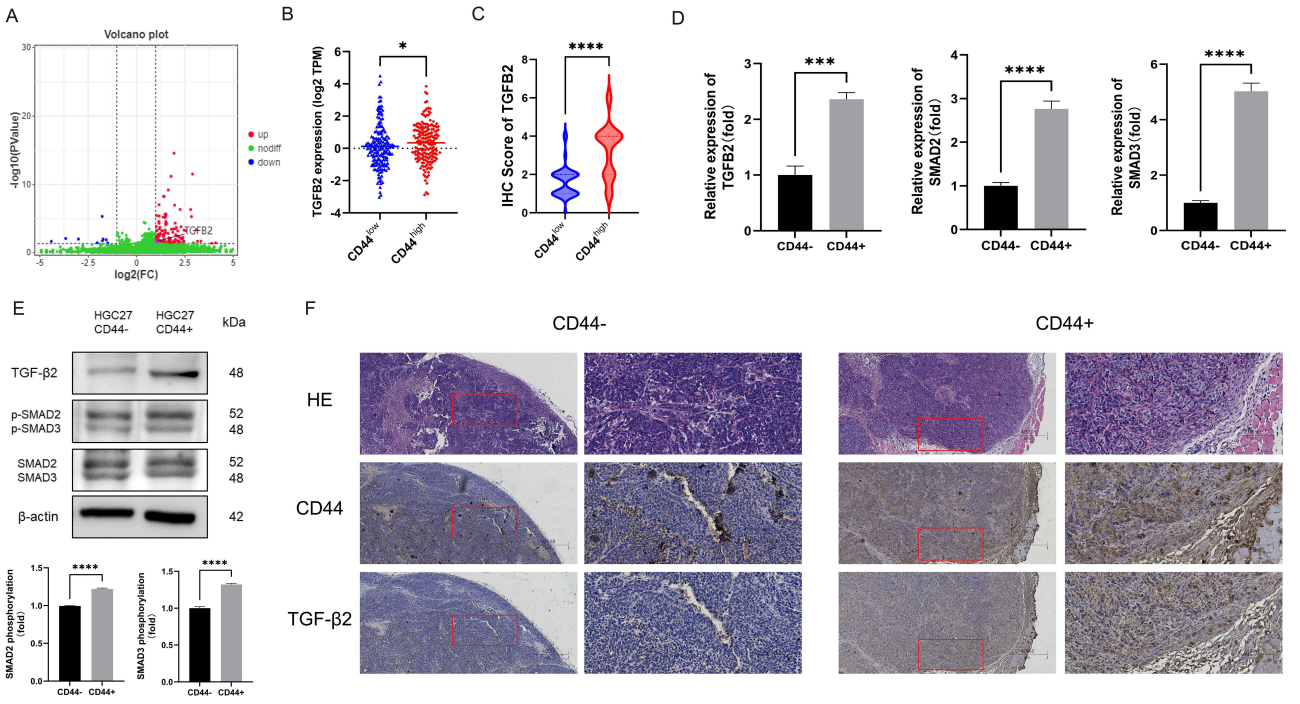

Figure 5 The TGF-β2/SMAD signalling pathway is upregulated in CD44+ cells. (**A**): Differential mRNAs between HGC27 CD44- and CD44+ cells were identified by sequencing, in which TGFB2 was upregulated in CD44+ cells. ($p < 0.05$) (**B**): Expression levels of TGFB2 between the two groups of samples with differential expression of CD44 in TCGA database. (*$p < 0.05$) (**C**): IHC staining scores for TGFB2 were significantly higher in CD44 high clinical samples than they were in CD44 low. (****$p < 0.0001$) (**D**): Real-time PCR analysis of the TGFB2, SMAD2, and SMAD3 expression level in HGC27 CD44- and CD44+ cells and they were normalized by GAPDH and presented as the relative ratio. (***$p < 0.001$, ****$p < 0.0001$) (**E**): Western blot analysis of TGF-β2, SMAD2/3, phosphorylated SMAD2/3 expression in CD44- and CD44+ cells. The above pathway proteins were activated in CD44+ cells. (****$p < 0.0001$) (**F**): The CD44- and CD44+ tumours inoculated in nude mice were stained with HE and IHC and observed at 50x and 200x field respectively.

score in the high CD44 group. (Figure 5C) Through in vitro experiments, we verified the gene and protein levels of TGFB2 and the downstream genes SMAD2 and SMAD3 and found that the TGF-β2/SMAD signalling pathway was activated in CD44+ cells. (Figure 5D and E) And the noticeable high expression of TGF-β2 in CD44+ group was also confirmed in vitro experiments. (Figure 5F)

Inhibition of miR-21-5p Decreases TGF-β2/SMAD Signalling Pathway Expression in CD44+ Cells

To study changes in CD44+ cells resulting from miR-21-5p expression, we transfected miR-21-5p inhibitor into CD44+ cells. At 48 hours posttransfection, we carried out real-time PCR to determine the expression level of miR-21-5p in CD44+ cells transfected with a negative control or the miR-21-5p inhibitor. We found that miR-21-5p expression was effectively downregulated by its inhibitor. (Figure 6A) Moreover, we observed that expression of TGFB2, a miR-21-5p target, decreased after the downregulation of miR-21-5p, and the same was observed for the downstream genes SMAD2 and SMAD3. (Figure 6B) Meanwhile, we found the same trend at the protein level. (Figure 6C) The above results demonstrated that the TGF-β2/SMAD signalling pathway may be a direct and specific target of miR-21-5p for regulatory functions in GCSCs.

Inhibition of miR-21-5p Increases the Cisplatin Sensitivity of CD44+ Cells

We tested the sensitivity of cisplatin in two groups of CD44+ cells transfected with a negative control (NC) or the miR-21-5p inhibitor by CCK-8 assays. Additionally, after 48 hours of treatment with different concentrations of cisplatin, the IC50 was significantly decreased in CD44+ cells treated with an inhibitor compared to NC cells. This indicated that reducing miR-21-5p can increase the sensitivity of CD44+ cells to cisplatin. (Figure 6D)

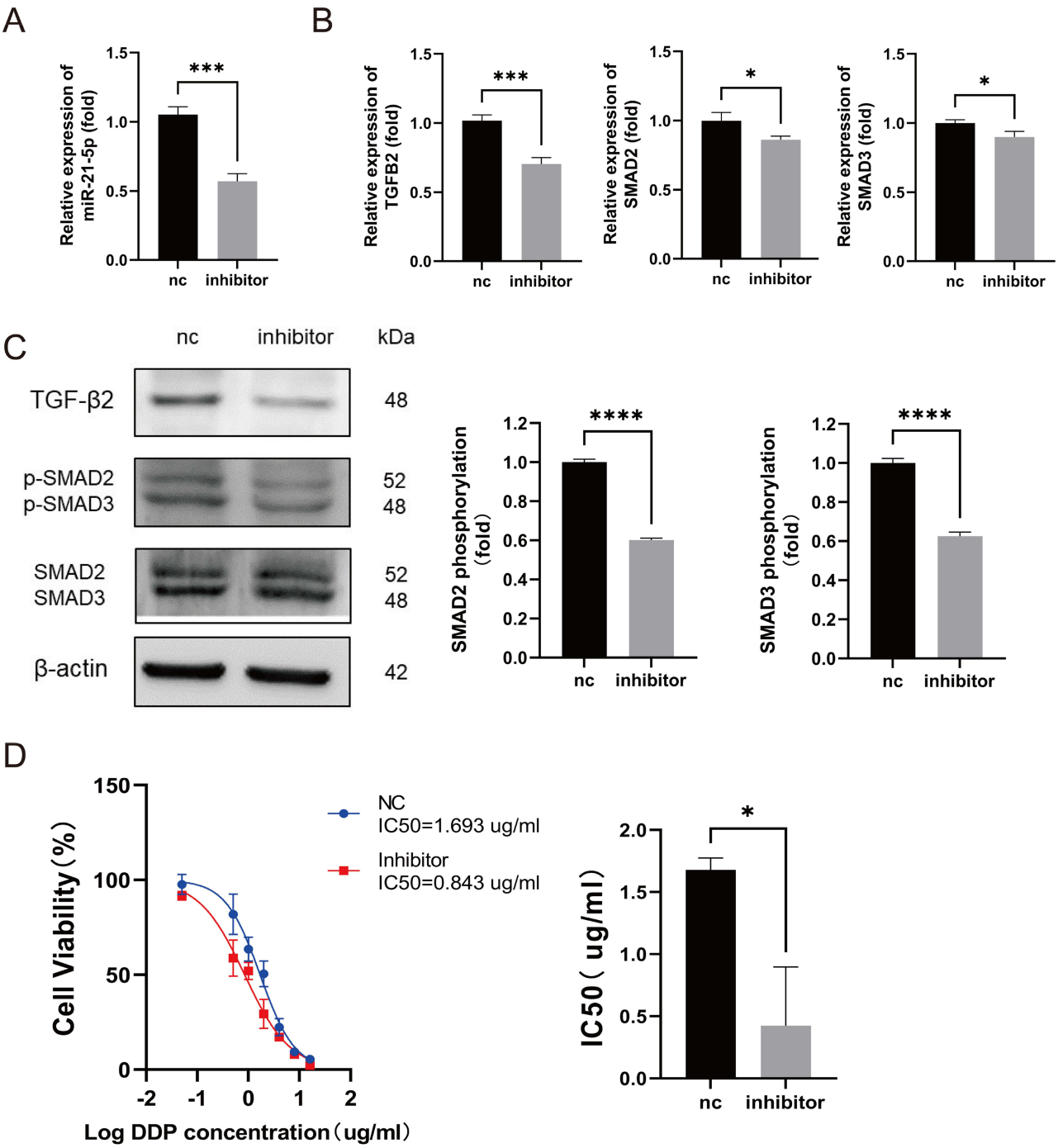

Figure 6 Inhibition of miR-21-5p decreases TGF-β2/SMAD signalling pathway expression in CD44+ cells. (**A**): CD44+ HGC27 cells were transfected with miR-21-5p inhibitor and negative control respectively, and there was significant inhibition by PCR detection. (***p < 0.001) (**B**): Real time PCR showed that the mRNA expression levels of TGFB2, SMAD2, SMAD3 all decreased with the inhibition of miR-21-5p. (*p < 0.05. ***p < 0.001) (**C**): TGF-β2/SMAD pathway protein levels decreased with miR-21-5p inhibition. (****p < 0.0001) (**D**): Cisplatin sensitivity in CD44+ HGC27 cells with native control (NC) and with miR-21-5p inhibitor. Viabilities of NC and inhibitor after treatment with different concentration cisplatin as measured by CCK8 assay. Values shown represent averages of half maximal inhibitory concentration; each treatment was carried out in triplicate (**p < 0.01).

Discussion

Although the incidence of gastric cancer (GC) is now declining, the mortality remains high. In addition to surgery, adjuvant chemotherapy is also an important treatment modality for gastric cancer patients. Cisplatin-based chemotherapy is now the most commonly used chemotherapeutic agent in GC. Cisplatin is considered a cytotoxic drug that kills cancer

cells by damaging DNA, inhibiting DNA synthesis and mitosis, and inducing apoptotic cell death.[29] Unfortunately, advanced GC patients who develop resistance to cisplatin currently have limited therapeutic options in the clinic.[30] Therefore, reducing the resistance of GC cells to cisplatin is a therapeutic target.

There is increasing evidence that tumours are composed of phenotypically and functionally diverse populations of neoplastic cells. Among them, cancer stem cells (CSCs) are defined as "cancer root cells" and have the ability for self-renew and proliferate into heterogeneous malignant stem cells and tumour cells that form the mass of the tumour. They are also considered to be one of the reasons for tumour chemotherapy resistance.[9] An Y et al[31] reported that SIRT1 inhibited cisplatin chemotherapy resistance by inhibiting GCSC properties. Yoon C et al[32] reported that Hedgehog pathway inhibition can reverse chemotherapy resistance in GCSCs. Therefore, therapeutic approaches targeting CSCs bring new hope for future antitumour treatment.

CD44 is a proven GCSC marker and is known to play a critical role in chemoresistance.[10] We performed flow sorting of the gastric cancer cell line HGC27 according to the expression of CD44, aiming to obtain GCSCs and negative controls. We validated CD44 expression between CD44- cells and CD44+ GCSCs at multiple levels and found significant differences between the two. After further culture, we found that GCSCs were significantly more resistant to cisplatin than CD44- cells both in vitro and in vivo. Yang et al pointed out that GCSC screened by CD133 had high cisplatin resistance, while Lee et al also proposed that CD44 + GCSC were highly resistant to cisplatin, which was verified in vivo and in vitro experiments.[33,34] Their conclusions also further support our inference.

RNA is probably the first macromolecule evolved in life and may play an important role in regulating cell functions. In addition to the well-known members such as tRNA, mRNA, and rRNA associated with the central dogma of genetics, several types of small RNAs, such as miRNAs, have recently been identified as key regulators of gene expression and cellular function.[35] miRNA regulation has previously been examined as a characteristic of CSCs. Therefore, we performed transcriptome sequencing of the above two cell lines. Among these differentially expressed miRNAs, we focused on miR-21-5p, which was significantly upregulated in CD44+ GCSCs compared with CD44- cells.

Although the role of miR-21-5p has remained largely uncharacterized, several studies have recently focused on this miRNA in various cancers. Tang J et al[36] reported that miR-21-5p may promote cell proliferation, migration and invasion in lung cancer cells. In gastric cancer, exosomal miR-21-5p induces mesothelial-to-mesenchymal transition and promotes peritoneal metastasis.[37] Chen J et al[26] indicated that miR-21-5p confers doxorubicin resistance in gastric cancer cells. However, the mechanism of the miR-21-5p-dependent cisplatin resistance response underlying gastric cancer stemness has not been fully elucidated.

In this regard, we analysed the targets of miR-21-5p and related signalling pathways and noted the gene TGFB2. We predicted that TGFB2 was the downstream target of miR-21-5p and played a role by regulating the TGF-β2 pathway through bioinformatics analysis. Luciferase experiments then showed that TGFB2 is indeed the downstream target gene of miR-21-5p. Multiple studies have recognized that the transforming growth factor beta (TGF-β) signalling pathway plays a crucial role in promoting metastasis in GC, and it can be activated by TGF-βs (TGF-β1, TGF-β2 and TGF-β3).[38,39] Recent studies have shown that TGFB2 is upregulated in GC and predicts poor survival.[40] TGF-βs can activate canonical TGFβ signalling and subsequently phosphorylate Smad2/3, which are the main intracellular effectors of the TGF-β pathway.[38] In the present study, we found that TGFB2 was also upregulated in GCSCs along with miR-21-5p. Whether in the TCGA database, in vivo experiments, or in vitro experiments, it showed significant high expression in the CD44+ group. Validation with our centre patients' data yielded the same result. Meanwhile, the TGF-β2/SMAD pathway regulated by TGFB2 showed the same trend.

Interestingly, in most studies, miRNAs play a negative regulatory role on target genes. After recent studies, the view that miRNAs can upregulate the expression of target genes has gradually been accepted by scholars. Vasudevan S et al[41] documented that miRNAs can induce translation upregulation of target mRNAs. Place RF et al[42] identified that miRNA-373 can target promoter sequences and induce gene expression. Huang V et al[43] revealed that multiple endogenous miRNAs activate Ccnb1 expression in mouse cells. In our study, miR-21-5p and the target gene TGFB2 showed a positive relationship, and the specific mechanism needs further exploration. This positive relationship was also proven by Di Bernardini E et al.[44]

In addition, this study is limited to the resistance of gastric cancer to cisplatin. In fact, many other types of drugs have also played an important role in the occurrence and development of gastric cancer and other tumours, which also reminds us of some more research directions. This is also the limitation of this paper and the space thinking for further consideration.[45,46]

In summary, to further validate our proposed inference, we knocked down miR-21-5p in GCSCs. Notably, knockdown of miR-21-5p made GCSCs less resistant to cisplatin. Meanwhile, the reduction in miR-21-5p levels led to the inhibition of the TGF-β2/SMAD pathway. In summary, we believe that miR-21-5p controls cisplatin resistance by regulating this pathway in GCSCs.

Conclusions

This study indicated that miR-21-5p plays an important role in cisplatin resistance in gastric cancer stem cells by regulating the TGF-β2/SMAD signalling pathway.

Data Sharing Statement

Gastric cancer data was downloaded from the TCGA database (https://tcga-data.nci.nih.gov/tcga/) under the accession number(s) gdc_download_20211208_042901.925377.

Ethics Approval and Consent to Participate

All participants provided written informed consent, and the study was approved by the Ethics Committee of Tianjin Medical University General Hospital (IRB2022-WZ-151, Tianjin China). This study was conducted in accordance with the Declaration of Helsinki. All animal assays were approved by the Institutional Animal Care and Research Advisory Committee of Tianjin Medical University (Tianjin, China) and performed in accordance with relevant guidelines and regulations (SYXK:2019-0004). This study was conducted following the Animal Research: Reporting of in vivo Experiments (ARRIVE) guidelines and the British Journal of Cancer (BJC) animal welfare guidelines (2010).

Consent for Publication

Written informed consent for publication of their clinical data was obtained from the patients.

Author Contributions

All authors made a significant contribution to the work reported, whether that is in the conception, study design, execution, acquisition of data, analysis and interpretation, or in all these areas; took part in drafting, revising or critically reviewing the article; gave final approval of the version to be published; have agreed on the journal to which the article has been submitted; and agree to be accountable for all aspects of the work.

Funding

This study is funded by the National Natural Science Foundation of China (No.82003301).

Disclosure

The all authors declare that the research was conducted in the absence of any commercial or financial relationships that could be construed as a potential conflict of interest.

References

1. Sung H, Ferlay J, Siegel RL, et al. Global cancer statistics 2020: GLOBOCAN estimates of incidence and mortality worldwide for 36 cancers in 185 countries. *CA Cancer J Clin*. 2021;71:209–249. doi:10.3322/caac.21660
2. Codd AS, Kanaseki T, Torigo T, Tabi Z. Cancer stem cells as targets for immunotherapy. *Immunology*. 2018;153:304–314. doi:10.1111/imm.12866
3. Zhang X, Hua R, Wang X, et al. Identification of stem-like cells and clinical significance of candidate stem cell markers in gastric cancer. *Oncotarget*. 2016;7:9815–9831. doi:10.18632/oncotarget.6890
4. Atashzar MR, Baharlou R, Karami J, et al. Cancer stem cells: a review from origin to therapeutic implications. *J Cell Physiol*. 2020;235:790–803. doi:10.1002/jcp.29044

5. Hancock RE, Siehnel R, Martin N. Outer membrane proteins of Pseudomonas. *Mol Microbiol*. 1990;4:1069–1075. doi:10.1111/j.1365-2958.1990.tb00680.x
6. Prager BC, Xie Q, Bao S, Rich JN. Cancer stem cells: the architects of the tumor ecosystem. *Cell Stem Cell*. 2019;24:41–53. doi:10.1016/j.stem.2018.12.009
7. Lau WM, Teng E, Chong HS, et al. CD44v8-10 is a cancer-specific marker for gastric cancer stem cells. *Cancer Res*. 2014;74:2630–2641. doi:10.1158/0008-5472.CAN-13-2309
8. Leon G, Macdonagh L, Finn SP, Cuffe S, Barr MP. Cancer stem cells in drug resistant lung cancer: targeting cell surface markers and signaling pathways. *Pharmacol Ther*. 2016;158:71–90. doi:10.1016/j.pharmthera.2015.12.001
9. Han J, Won M, Kim JH, et al. Cancer stem cell-targeted bio-imaging and chemotherapeutic perspective. *Chem Soc Rev*. 2020;49:7856–7878. doi:10.1039/d0cs00379d
10. Thapa R, Wilson GD. The Importance of CD44 as a stem cell biomarker and therapeutic target in cancer. *Stem Cells Int*. 2016;2016:2087204. doi:10.1155/2016/2087204
11. Walcher L, Kistenmacher AK, Suo H, et al. Cancer stem cells-origins and biomarkers: perspectives for targeted personalized therapies. *Front Immunol*. 2020;11:1280. doi:10.3389/fimmu.2020.01280
12. Rabik CA, Dolan ME. Molecular mechanisms of resistance and toxicity associated with platinating agents. *Cancer Treat Rev*. 2007;33:9–23. doi:10.1016/j.ctrv.2006.09.006
13. Webb A, Cunningham D, Scarffe JH, et al. Randomized trial comparing epirubicin, cisplatin, and fluorouracil versus fluorouracil, doxorubicin, and methotrexate in advanced esophagogastric cancer. *J Clin Oncol*. 1997;15:261–267. doi:10.1200/JCO.1997.15.1.261
14. Compare D, Rocco A, Nardone G. Risk factors in gastric cancer. *Eur Rev Med Pharmacol Sci*. 2010;14:302–308.
15. Garcia-Mayea Y, Mir C, Masson F, Paciucci R, Me LL. Insights into new mechanisms and models of cancer stem cell multidrug resistance. *Semin Cancer Biol*. 2020;60:166–180. doi:10.1016/j.semcancer.2019.07.022
16. Szakacs G, Paterson JK, Ludwig JA, Booth-Genthe C, Gottesman MM. Targeting multidrug resistance in cancer. *Nat Rev Drug Discov*. 2006;5:219–234. doi:10.1038/nrd1984
17. Yingling JM, Blanchard KL, Sawyer JS. Development of TGF-beta signalling inhibitors for cancer therapy. *Nat Rev Drug Discov*. 2004;3:1011–1022. doi:10.1038/nrd1580
18. Mens MMJ, Ghanbari M. Cell cycle regulation of stem cells by MicroRNAs. *Stem Cell Rev Rep*. 2018;14:309–322. doi:10.1007/s12015-018-9808-y
19. Pan Y, Shu X, Sun L, et al. miR196a5p modulates gastric cancer stem cell characteristics by targeting Smad4. *Int J Oncol*. 2017;50:1965–1976. doi:10.3892/ijo.2017.3965
20. Takahashi RU, Miyazaki H, Ochiya T. The role of microRNAs in the regulation of cancer stem cells. *Front Genet*. 2014;4:295. doi:10.3389/fgene.2013.00295
21. Ma C, Huang T, Ding YC, et al. MicroRNA-200c overexpression inhibits chemoresistance, invasion and colony formation of human pancreatic cancer stem cells. *Int J Clin Exp Pathol*. 2015;8:6533–6539.
22. Tao L, Wu YQ, Zhang SP. MiR-21-5p enhances the progression and paclitaxel resistance in drug-resistant breast cancer cell lines by targeting PDCD4. *Neoplasma*. 2019;66:746–755. doi:10.4149/neo_2018_181207N930
23. Chen S, Yang C, Sun C, et al. miR-21-5p suppressed the sensitivity of hepatocellular carcinoma cells to cisplatin by targeting FASLG. *DNA Cell Biol*. 2019;38:865–873. doi:10.1089/dna.2018.4529
24. Bica-Pop C, Cojocneanu-Petric R, Magdo L, et al. Overview upon miR-21 in lung cancer: focus on NSCLC. *Cell Mol Life Sci*. 2018;75:3539–3551. doi:10.1007/s00018-018-2877-x
25. Das PK, Islam F, Lam AK. The roles of cancer stem cells and therapy resistance in colorectal carcinoma. *Cells*. 2020;9:1392. doi:10.3390/cells9061392
26. Chen J, Zhou C, Li J, et al. miR215p confers doxorubicin resistance in gastric cancer cells by targeting PTEN and TIMP3. *Int J Mol Med*. 2018;41:1855–1866. doi:10.3892/ijmm.2018.3405
27. Zheng P, Chen L, Yuan X, et al. Exosomal transfer of tumor-associated macrophage-derived miR-21 confers cisplatin resistance in gastric cancer cells. *J Exp Clin Cancer Res*. 2017;36:53. doi:10.1186/s13046-017-0528-y
28. Singh A, Singh AK, Giri R, et al. The role of microRNA-21 in the onset and progression of cancer. *Future Med Chem*. 2021;13:1885–1906. doi:10.4155/fmc-2021-0096
29. Dasari S, Tchounwou PB. Cisplatin in cancer therapy: molecular mechanisms of action. *Eur J Pharmacol*. 2014;740:364–378. doi:10.1016/j.ejphar.2014.07.025
30. Orditura M, Galizia G, Sforza V, et al. Treatment of gastric cancer. *World J Gastroenterol*. 2014;20:1635–1649. doi:10.3748/wjg.v20.i7.1635
31. An Y, Wang B, Wang X, et al. SIRT1 inhibits chemoresistance and cancer stemness of gastric cancer by initiating an AMPK/FOXO3 positive feedback loop. *Cell Death Dis*. 2020;11:115. doi:10.1038/s41419-020-2308-4
32. Yoon C, Park DJ, Schmidt B, et al. CD44 expression denotes a subpopulation of gastric cancer cells in which Hedgehog signaling promotes chemotherapy resistance. *Clin Cancer Res*. 2014;20:3974–3988. doi:10.1158/1078-0432.CCR-14-0011
33. Han Y, Sun B, Cai H, Xuan Y. Simultaneously target of normal and stem cells-like gastric cancer cells via cisplatin and anti-CD133 CAR-T combination therapy. *Cancer Immunol Immunother*. 2021;70:2795–2803. doi:10.1007/s00262-021-02891-x
34. Lee SD, Yu D, Lee DY, et al. Upregulated microRNA-193a-3p is responsible for cisplatin resistance in CD 44 (+) gastric cancer cells. *Cancer Sci*. 2019;110:662–673. doi:10.1111/cas.13894
35. Wang S, Li MY, Liu Y, et al. The role of microRNA in cisplatin resistance or sensitivity. *Expert Opin Ther Targets*. 2020;24:885–897. doi:10.1080/14728222.2020.1785431
36. Tang J, Li X, Cheng T, Wu J. miR-21-5p/SMAD7 axis promotes the progress of lung cancer. *Thorac Cancer*. 2021;12:2307–2313. doi:10.1111/1759-7714.14060
37. Li Q, Li B, Li Q, et al. Exosomal miR-21-5p derived from gastric cancer promotes peritoneal metastasis via mesothelial-to-mesenchymal transition. *Cell Death Dis*. 2018;9:854. doi:10.1038/s41419-018-0928-8
38. Colak S, Ten Dijke P. Targeting TGF-beta signaling in cancer. *Trends Cancer*. 2017;3:56–71. doi:10.1016/j.trecan.2016.11.008
39. Song C, Zhou C. HOXA10 mediates epithelial-mesenchymal transition to promote gastric cancer metastasis partly via modulation of TGFB2/Smad/METTL3 signaling axis. *J Exp Clin Cancer Res*. 2021;40:62. doi:10.1186/s13046-021-01859-0

40. Yang B, Bai J, Shi R, et al. TGFB2 serves as a link between epithelial-mesenchymal transition and tumor mutation burden in gastric cancer. *Int Immunopharmacol*. 2020;84:106532. doi:10.1016/j.intimp.2020.106532
41. Vasudevan S, Tong Y, Steitz JA. Switching from repression to activation: microRNAs can up-regulate translation. *Science*. 2007;318:1931–1934. doi:10.1126/science.1149460
42. Place RF, Li LC, Pookot D, Noonan EJ, Dahiya R. MicroRNA-373 induces expression of genes with complementary promoter sequences. *Proc Natl Acad Sci U S A*. 2008;105:1608–1613. doi:10.1073/pnas.0707594105
43. Huang V, Place RF, Portnoy V, et al. Upregulation of Cyclin B1 by miRNA and its implications in cancer. *Nucleic Acids Res*. 2012;40:1695–1707. doi:10.1093/nar/gkr934
44. Di Bernardini E, Campagnolo P, Margariti A, et al. Endothelial lineage differentiation from induced pluripotent stem cells is regulated by microRNA-21 and transforming growth factor beta2 (TGF-beta2) pathways. *J Biol Chem*. 2014;289:3383–3393. doi:10.1074/jbc.M113.495531
45. Gao S, Tan H, Gang J, et al. Inhibition of hepatocellular carcinoma cell proliferation through regulation of the cell cycle, AGE-RAGE, and leptin signaling pathways by a compound formulation comprised of andrographolide, wogonin, and oroxylin A derived from Andrographis paniculata (Burm.f.) Nees. *J Ethnopharmacol*. 2024;329:118001. doi:10.1016/j.jep.2024.118001
46. Gao S, Tan H, Li D. Oridonin suppresses gastric cancer SGC-7901 cell proliferation by targeting the TNF-alpha/androgen receptor/TGF-beta signalling pathway axis. *J Cell Mol Med*. 2023;27(18):2661–2674. doi:10.1111/jcmm.17841